Attitude Dynamics and Control of an Apogee Motor Assembly with Paired Satellites

MARSHALL H. KAPLAN* AND NORMAN M. BECK JR.†
The Pennsylvania State University, University Park, Pa.

The Apogee Motor Assembly with Paired Satellites (AMAPS) technique takes advantage of a well-known instability of spinning bodies to deploy pairs of satellites into high-circular orbits from either a low-orbiting space shuttle or a launch vehicle which performs the apogee transfer injection. A spinning semirigid body, free of applied torques and active controls, is stable only when rotating about its axis of maximum moment of inertia, because energy dissipates until a minimum energy state is reached. This principle has been widely used in the passive attitude control of Earth satellites and has been disastrous to those who ignored it. In this application, the instability associated with rotation about the minor principal axis is used to passively control spin axis reorientation of the payload assembly. An investigation of associated attitude dynamics and energy dissipation processes is reported here. Dissipation is simulated with viscous ring dampers. Approximate and numerical methods for predicting time of spin axis reorientation from minor to major principal axis are reviewed and examples presented.

Nomenclature

A, B, C = principal moments of inertia of the rigid body
D = diameter of ring cross section
f = Darcy-Wiesbach resistance coefficient
h_x, h_y, h_z = components of angular momentum about the body-fixed axes
I_x, I_y, I_z = moments of inertia of the fluid slug about the body-fixed axes
N_z = moment due to viscous shear in the annular ring
P = circumference of the ring cross section
Q_α = generalized torque function
R = mean radius of the viscous ring
R_n = Reynolds number $= RD\dot{\alpha}/\nu$
S = cross-sectional area of viscous ring
T = rotational kinetic energy
v = velocity of the fluid slug relative to the ring
$\alpha, \dot{\alpha}$ = angular position and velocity of fluid slug relative to the ring, respectively
β = angular span of fluid slug in the ring
ν, ρ = kinematic viscosity and density of damper fluid, respectively
τ_0 = shear stress
ϕ, θ, ψ = Euler angles
ω_0 = initial spin rate about Z-direction
$\omega_x, \omega_y, \omega_z$ = components of angular velocity about the body-fixed axes

Introduction

A SPINNING semirigid body, free of applied torques and active controls is stable only when rotating about its axis of maximum moment of inertia. This phenomenon has been widely used advantageously for passive attitude control of Earth satellites, but has proven disastrous to those who have ignored it.[1] Explorer I is a classic example of the consequences of such a neglect. After only a few hours into the flight of the first American satellite, radio signals indicated a tumbling motion had developed and was increasing in amplitude in an unstable manner. It was concluded that the four turnstile wire antennae were dissipating energy; thus, causing a transfer of body spin axis from the axis of minimum moment of inertia to a transverse axis.[2] The Apogee Motor Assembly with Paired Satellites (AMAPS) technique uses this instability to passively transform spin axis orientation during deployment of a pair of satellites into high-circular orbits from either a low-orbiting space shuttle or a launch vehicle which performs the apogee transfer injection. The use of this technique with a surface-to-orbit shuttle system would eliminate the requirement for an orbit-to-orbit shuttle; thus, permitting the use of relatively simple deployment hardware. Active attitude control beyond apogee transfer injection is not required when the AMAPS scheme is used with a launch vehicle or shuttle. Furthermore, the requirement for built-in apogee kick motors as part of the satellites is eliminated.

Primary objectives of this study are to develop the AMAPS scheme and investigate methods for analytically determining spin axis transfer times for realistic satellite configurations. Energy dissipation is provided by a viscous ring damper mounted on the major axis. Solutions of attitude motion for large angle reorientation of asymmetric spacecraft are not generally available and must be obtained with approximate or numerical methods. When the axis of maximum moment of inertia is oriented close to the angular momentum direction, linearization is possible and results are available in the literature for such cases.[3] Feasibility of the scheme is discussed and numerical examples are presented.

Operational Schemes

There are two basic configurations with which the AMAPS technique may be associated. When used with a launch vehicle no apogee transfer injection motor is required. Such a scheme is illustrated in Fig. 1. Either the upper stage of the booster is spin stabilized, or a spin table is used to spin-up AMAPS about the YY-axis. Immediately after injection into a high-altitude transfer orbit the payload attitude is changed so that the momentum vector is reoriented for later apogee firings, and then the release sequence is executed. Since the assembly is stable about its axis of maximum moment of inertia, energy dissipation would result in the transfer of spin to the axis of maximum moment of inertia while keeping the direction of the angular momentum vector fixed in inertial

Presented as Paper 71-953 at the AIAA Guidance, Control and Flight Mechanics Conference, Hofstra University, Hempstead, N.Y., August 16–18, 1971; submitted September 7, 1971; revision received January 28, 1972. The work reported here is being supported under NASA Grant NGR 39-009-162.

Index category: Spacecraft Attitude Dynamics and Control.

* Assistant Professor of Aerospace Engineering. Associate Fellow AIAA.

† Former Graduate Assistant; now a Second Lieutenant, USAF.

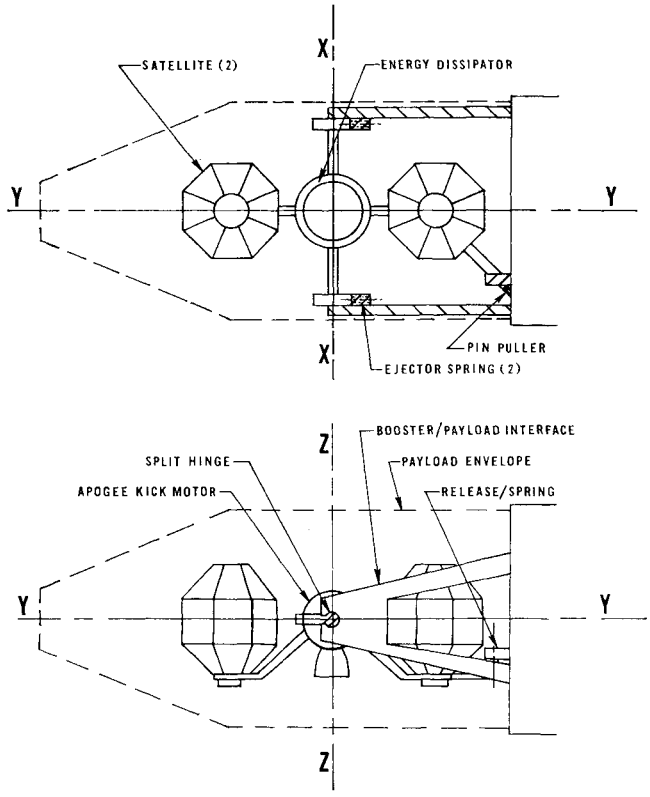

Fig. 1 AMAPS configuration for launch vehicle applications.

space. It is assumed that the ZZ-axis is the body axis of maximum moment of inertia and YY is the axis of minimum moment of inertia. The ZZ-axis will tend to align itself with the angular moment direction if the YY-axis is initially perturbed when separated from the launch vehicle, and the assembly has an energy absorber or nutation damper. Figure 1 shows how initial conditions can be achieved in order to start the transfer of the rotation axis as the assembly leaves the launch vehicle. Immediately after injection into apogee transfer by the upper stage, a pin puller device is fired. This allows a spring to start rotational motion about the XX-axis, which induces a perturbation, starting the transfer of rotation axes. When the split hinges line up with the axle flats, springs will push the assembly away from the upper stage, and the payload is then freely precessing. The axially mounted damper shown in Fig. 1 will absorb energy in such a way as to transfer spin axes. The rate of axis transfer for a given payload is a function of initial spin rate and the energy dissipator configuration. When the assembly has stabilized and is rotating only about the ZZ-axis, then this axis will be parallel to the original YY-direction, and the assembly will be in the proper orientation for apogee firing. After apogee kick, the two satellites can be separated and, if desired, spun up

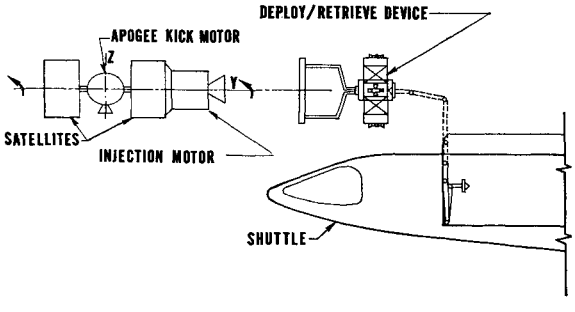

Fig. 2 AMAPS package leaving deploy/retrieve device.

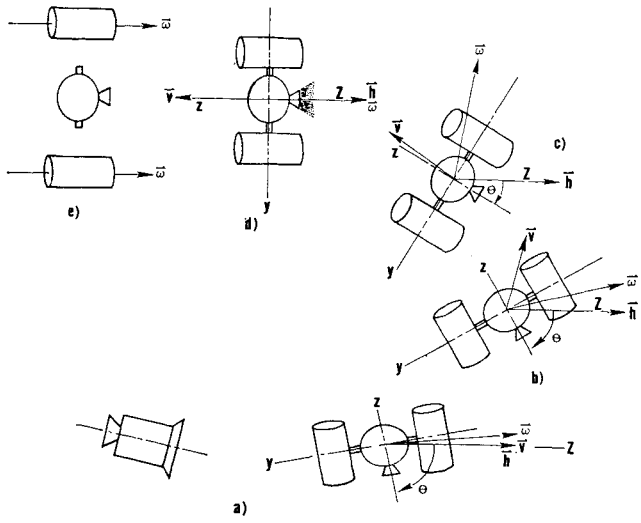

Fig. 3 Deployment sequence for shuttle scheme.

simultaneously by converting angular momentum of the assembly to the satellites. Spin rate adjustments and positioning around the orbit can be done with individual satellite propulsion systems.

The other basic configuration useful with the AMAPS technique is associated with deployment from a low-orbiting space shuttle. This scheme is illustrated in Fig. 2. The payload package consists of two satellites, an apogee kick motor, and an apogee transfer injection motor. This assembly is deployed from the cargo bay and spun up about the Y-axis by a deploy/retrieve device.[4] The payload package is then separated from this device, and the apogee transfer motor is fired shortly thereafter. This is followed by reorientation with the limited attitude control capability of the injection motor subsystem, and then payload separation and perturbation occur. The apogee transfer and axis transformation sequence is shown schematically in Fig. 3.

Discussion of the Problem

The time of transfer of spin axes from the axis of minimum to maximum moment of inertia is a function of energy dissipation rate. This, in turn, depends on the orientation and magnitude of angular momentum for a given AMAPS configuration and absorber. The most accurate approach to determining this time is to simulate the free body motion with energy dissipation over the time interval of interest. Since the axis transformation time should be less than or equal to the time of transfer to apogee (typically about 5 hr), this situation could be represented by a two point boundary value problem with fixed terminal time. However, the end conditions on orientation are satisfied naturally by the effects of dissipation. Thus, the motion can be conveniently treated as an initial value problem with an inequality constraint on axis transfer time, i.e., axis transfer time $\leq$ transfer to apogee time. Simulation of motion can be appropriately accomplished on a digital computer. However, the large number of iterations leads to practical limitations on the extent of quantitative results obtainable. Therefore, numerical simulations were carried to the point where feasibility of the scheme was satisfied.

Previous research of primary interest to this study is that which is related to fluid loop damper performance. A comparison of viscous and inertial forces acting on the fluid slug will determine whether motion in the ring is laminar or turbulent. The small angle (perturbation of stable spin state) case corresponds to laminar flow, because this situation is associated with high viscous and low-inertial forces along the

tangential direction. Small angle theory permits the fluid to be modeled as a closed ring, illustrated in Fig. 4. Energy is dissipated by cyclic forming and degeneration of surface waves. Fitzgibbon and Smith[3] have developed an energy dissipation function which accounts for this phenomenon. Furthermore, for large angle situations (significant deviation from stable spin about the axis of maximum moment of inertia) they conclude that turbulent flow must be assumed for θ greater than about 0.2 radians. Under these conditions the fluid forms a slug, also illustrated in Fig. 4. Motion of the slug with respect to the ring causes energy dissipation through shear stress acting on the wall of the tube, as in elementary pipe flow

$$\tau_0 = (f/4)\rho v^2/2$$

End effects are of negligible significance. However, the diameter of the cross section is restricted to be small compared with the ring radius in order to simplify integration of the shear stress over the wetted area of the ring. The retarding torque about the ring axis of symmetry becomes

$$N_z = -\tau_0(R^2 P\beta)$$

Therefore, the energy-dissipation rate is

$$\dot{T} = N_z\dot{\alpha} = -\tau_0 R^2 P\beta\dot{\alpha}$$

For turbulent flow ($2000 < R_n < 10^5$) in smooth round pipes, the resistance coefficient can be approximated by an empirical relation of Blasius

$$f = 0.316/R_n^{1/4}$$

Thus, the energy dissipation rate becomes

$$\dot{T} = -(0.316\rho P\beta R^4/8R_n^{1/4})\dot{\alpha}^3$$

$$= -0.0395[\rho P\beta R^{15/4}/(D/\nu)^{1/4}]\dot{\alpha}^{11/4}$$

This analytical formulation yielded good correlation with experiment for a 12° deviation of θ and was used for all values above 10°. As θ is reduced below 10° and approaches approximately 5°, neither large nor small angle theory holds. A realistic model of the fluid in this transistion phase is not yet available, because the fluid exhibits both laminar and turbulent properties over varying transition periods. To insure validity of large angle theory, it should be applied only for $\theta \geq 10°$.

A great deal of insight into the problem can be gained by summarizing available and experimental results related to spin axis reorientation. Consider a typical AMAPS configuration with initial spin about its minor axis and θ perturbed away from 90°. The rate of energy dissipation is very low for a considerable period of time, because the average fluid slug velocity is low. As θ decreases below about 75°, this velocity increases on the average; thus, increasing the energy loss rate and further promoting transition of spin axes. In fact, the mean value of θ is a parabolic function of time for large

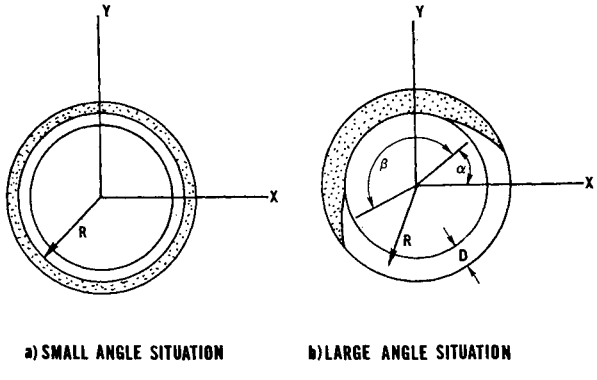

Fig. 4 Fluid configurations of interest.

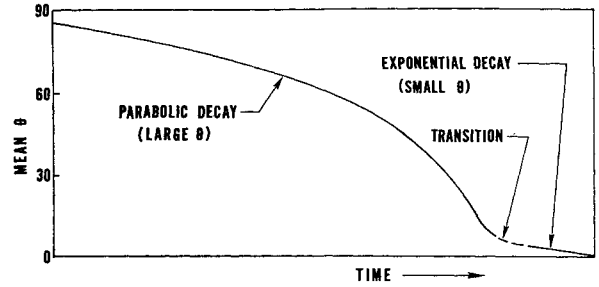

Fig. 5 Axis transformation phases.

values. The transition processes, as depicted in Fig. 5, can be modeled by large angle theory down to about $\theta = 10°$. Below about 5° small angle theory can be applied. Here an exponential decay is caused by the fluid loop. However, this period of time is shortened by added dissipation from vehicle flexibility and liquid sloshing in propellant tanks. Thus, the major portion of time for spin axis transformation is required to reduce the mean value of θ to about 10°.

Analytical Development

Solution of the equations of motion for a rigid body are readily available in the literature. Incorporation of a fluid loop damper about an initially transverse axis of an asymmetric body represents a situation not previously treated analytically with accurate simulation of dynamics. Thus, the equations of motion must be formulated to account for energy dissipation through a viscous mechanism and solved numerically for large values of θ. There are several distinct methods offered in the literature for developing these equations. They include the energy sink method,[5] discrete parameter model method, and modal model method.[6] The first, as the name infers, assumes dissipation by friction or viscous effects. It is perhaps the easiest to apply but requires approximations that sometimes cannot be rigorously justified and may produce erroneous results. The discrete parameter method employs rigorous forms of the equations of motion which are generally integrated by numerical methods. The modal model method is the most complex of the three. Of these methods the first and second were considered to be suitable for this study, and both are discussed below. However, the discrete parameter method was used in obtaining numerical results in order to insure accuracy and because this technique has proven useful with nutation dampers.[7]

The viscous ring dissipator was chosen because it has no moving mechanical parts, as do pendulum dampers or spring-mass-dashpot systems. Furthermore, such devices have been flight tested for spin axis reorientation with the WRESAT spacecraft.[8] The formulation of dynamics must account for this dissipation mechanism while maintaining constant angular momentum of the system. The following developments satisfy this condition.

Figure 6 shows the set of generalized coordinates used here: ϕ, θ, and ψ. Also, X, Y, Z and x, y, z are inertial and body-fixed coordinates, respectively. Note $\dot{\phi}$ is the precession rate and the net value of $\dot{\theta}$ is the induced nutation rate due to dissipation. General assumptions made in the analysis are: 1) The body is assumed rigid so that energy dissipation due to flexibility is neglected; and 2) The products of inertia of the fluid slug about axes parallel to the body principal axes are small relative to body moments of inertia and their effects can be neglected.

For the energy sink method, the body is assumed to be in force-free motion. During each revolution of ψ a certain amount of energy is lost due to viscous dissipation. This is easily modeled through conservation of angular momentum, i.e., the inertial components of this vector must be constant

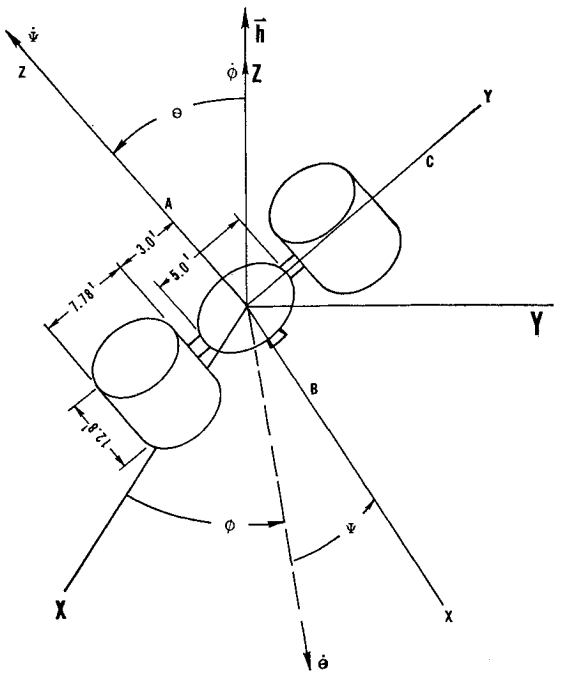

Fig. 6 Coordinate system and numerical model.

This is satisfied for AMAPS when $h_X = h_Y = 0$, and $h_Z = C\omega_0$. Very restrictive assumptions must also be made on the relative motion between the fluid slug and ring. For example, Fitzgibbon and Smith[3] assumed $\dot{\alpha} = \dot{\psi}$. Results can be obtained by computing an average $\dot{\psi}$ during a cycle of ψ and obtain the corresponding loss of energy during the interval of that cycle. A plot of $\dot{T}$ vs θ can be obtained, and numerical integration used to generate approximate curves of θ vs t for various situations. However, the validity of assuming $\dot{\alpha} = \dot{\psi}$ is questionable.

The discrete parameter model method uses the rigid body equations of motion to satisfy conservation of angular momentum. These are quickly expressible in the Euler form for principal axes[9]

$$\dot{h}_x + \omega_y h_z - \omega_z h_y = 0, \quad \dot{h}_y + \omega_z h_x - \omega_x h_z = 0,$$
$$\dot{h}_z + \omega_x h_y - \omega_y h_x = 0$$

Angular momentum components for the complete system are

$$h_x = (B + I_x)\omega_x, \qquad h_y = (C + I_y)\omega_y, \qquad h_z = A\omega_z + I_z(\omega_z + \dot{\alpha})$$

Note that the AMAPS configuration requires that $A > B > C$. Components of angular velocity can be expressed in terms of Euler angles by using standard transformations. To simulate energy dissipation, the fluid slug is modeled separately and as though acted upon by an outside viscous force. Thus, a generalized torque function Q_α can be introduced, and motion of this fluid body relative to the ring can be derived from a Lagrangian formulation,[10] as though it were a rigid body,

$$(d/dt)(\partial T/\partial\dot{\alpha}) - \partial T/\partial\alpha = Q_\alpha$$

Since Q_α is the retarding torque resulting from viscous shear, it must satisfy $Q_\alpha = N_z$. This technique could accommodate several such energy absorbers. However, only one annular ring is assumed here. This device is mounted about the body z-axis with its center at the center of mass of the assembly. The rotational kinetic energy of the fluid slug in terms of Euler's angles and angle rates is

$$T = (I_x/2)(\dot{\phi}\sin\theta\sin\psi + \dot{\theta}\cos\psi)^2 +$$
$$(I_y/2)(\dot{\phi}\sin\theta\cos\psi - \dot{\theta}\sin\psi)^2 + (I_z/2)(\dot{\psi} + \dot{\alpha} + \dot{\phi}\cos\theta)^2$$

Moments of inertia for the fluid slug were taken as

$$I_x = (\rho SR^3/4)[2\beta - \sin2(\alpha + \beta) + \sin2\alpha]$$
$$I_y = (\rho SR^3/4)[2\beta + \sin2(\alpha + \beta) - \sin2\alpha]$$
$$I_z = \rho S\beta R^3$$

The equations of motion for a rigid body with viscous energy dissipation become

$$(B + I_x)(\ddot{\phi}\sin\theta\sin\psi + \dot{\phi}\dot{\theta}\cos\theta\sin\psi + \dot{\phi}\dot{\psi}\sin\theta\cos\psi + \ddot{\theta}\cos\psi - \dot{\theta}\dot{\psi}\sin\psi) + \omega_x\dot{I}_x + \omega_y\omega_z A + \omega_y I_z(\omega_z + \dot{\alpha}) - \omega_z\omega_y(C + I_y) = 0$$

$$(C + I_y)(\ddot{\phi}\sin\theta\cos\psi + \dot{\phi}\dot{\theta}\cos\theta\cos\psi - \dot{\theta}\dot{\psi}\sin\theta\sin\psi - \ddot{\theta}\sin\psi - \dot{\theta}\dot{\psi}\cos\psi) + \omega_y\dot{I}_y + \omega_z\omega_x(B + I_x) - \omega_x\omega_z A - \omega_x I_z(\omega_z + \dot{\alpha}) = 0$$

$$A(\ddot{\psi} + \ddot{\phi}\cos\theta - \dot{\phi}\dot{\theta}\sin\theta) + I_z(\ddot{\psi} + \ddot{\phi}\cos\theta - \dot{\phi}\dot{\theta}\sin\theta + \ddot{\alpha}) + \omega_x\omega_y(C + I_y) - \omega_y\omega_x(B + I_x) = 0$$

$$I_z(\ddot{\psi} + \ddot{\alpha} + \ddot{\phi}\cos\theta - \dot{\phi}\dot{\theta}\sin\theta) - (\omega^2{}_x/2)\partial I_x/\partial\alpha - (\omega^2{}_y/2)\partial I_y/\partial\alpha + [0.316\rho P\beta R^{15/4}/8(D/\nu)^{1/4}]\dot{\alpha}^{7/4} = 0$$

The first three equations guarantee conservation of angular momentum while the last one supplies energy dissipation. This method provides greater accuracy, because relative fluid slug motion is not restrictive as in the energy sink formulation.

Discussion of Simulation Results

The discrete parameter model formulation presented above was applied to a numerical example. Integration was carried out for specified accuracy until error accumulation exceeded bound values. The large number of integration steps required to accurately simulate rotational motion severely limits the length of real time motion simulation. However, results for short time simulations indicate validity of this modeling method and provide a basis for determining whether or not axis transformation will be completed in the apogee transfer interval.

The large number of physical and dynamic parameters force a limitation on variations of these quantities for meaningful simulations. Consider an assembly consisting of two cylindrical satellites similar in shape and size to Intelsat IV and an ellipsoidal apogee kick motor, as shown in Fig. 6. The principal moments of inertia of the assembly are taken as

$$A = 6{,}920 \text{ lb-ft-sec}^2, \quad B = 5{,}190 \text{ lb-ft-sec}^2$$
$$C = 1{,}785 \text{ lb-ft-sec}^2$$

For the cases studied, mercury was selected for the viscous fluid, although other fluids can also be used, e.g., silicone. The pertinent physical properties of mercury are

$$\rho = 1.27 \times 10^{-3} \text{ lb-sec}^2/\text{in.}^4, \quad \nu = 1.8 \times 10^{-4} \text{ in.}^2/\text{sec}$$

The radius of the fluid loop was limited by several restrictions. In order to guarantee significant damping, R must be at least 3 ft. However, to neglect the products of inertia of the fluid slug when considering the dynamics of the rigid body, R was restricted to a maximum of 4.35 ft. For the

Table 1 Case variation of simulation parameters

Case	ω_0 (rad/min)	R (ft)	β (rad)
A	7.5	3.26	5.0
B	7.5	3.26	1.0
C	5.5	3.26	1.0
D	9.5	4.35	5.0
E	7.5	4.35	5.0
F	20.0	3.26	5.0
G	40.0	3.26	5.0
H	60.0	3.26	5.0
I	20.0	4.35	5.0
J	40.0	4.35	5.0
K	60.0	4.35	5.0

cases studied, R was taken as 3.26 and 4.35 ft and other parameters were varied for given R. Furthermore, in the analysis of viscous energy dissipation, straight pipe flow was assumed. This leads to the restriction that the cross-sectional radius of the ring must not be greater than 3% of the ring radius. In all cases studied, the cross-sectional radius was held at 3% for maximum damping.

Two different enclosed angles of the fluid slug were considered, $\beta = 1.0$ radian and $\beta = 5.0$ radians. There was, of course, no limit on initial spin rate. However, as ω_0 was increased, real time simulation was decreased due to associated increases in all other dynamic parameters. This then led to earlier breakdown in accuracy limitations for the simulation. Thus, ω_0 was restricted to a maximum of 60 rad/min. Assuming the configuration to be restricted as outlined, parameters which effect energy dissipation and the mean value of the nutation angle θ, were varied as listed in Table 1.

The rate of kinetic energy dissipation is of primary importance. Fig. 7 offers curves of energy vs time for two values of ω_0 at $\beta = 1.0$ rad. Computations were obtained for 80 mins of real time for cases B and C. By comparison case B, with greater initial spin, has greater dissipation and loss rate than case C. However, greater initial spin implies more energy must be dissipated. The parameter of interest is the percent of energy dissipated of the total energy to be dissipated in given time. Case B dissipated approximately 32% of the total energy to be lost while case C dissipated only 8% in the same 80 min. Case D and E yielded analogous results. Thus, a greater initial spin rate seems to result in faster axis transformation, even though there is more energy to be dissipated. This greater rate of loss of kinetic energy for increased ω_0 can be attributed to the increase in dynamic rates. As spin rate increases the average relative velocity of the fluid slug with respect to the ring will also increase, thus, increasing energy dissipation.

The effect of varying the fluid slug size can be considered by comparing the curve of case A for $\beta = 5$ rad with that of case B of Fig. 7. Case A has dissipated 13% of energy in

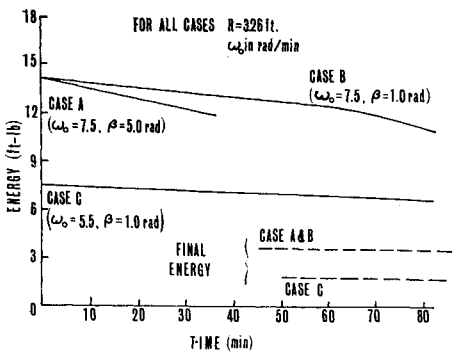

Fig. 7 Energy dissipation profiles.

Table 2 Percent decrease in kinetic energy for various cases during 30 min of real time

Case	ω_0 (rad/min)	Percent decrease in energy	R (ft)
F	20	37	3.26
G	40	46	3.26
H	60	51	3.26
I	20	40	4.35
J	40	50	4.35
K	60	58	4.35

30 min and extrapolation to 82 min indicates it will dissipate about 35%. As expected, increasing β results in increased dissipation rates.

Cases F to K were simulated for an equivalent of 30 min for initial spin rates of 20, 40, and 60 rad/min. These verify the earlier results, i.e., the rate of energy dissipation increases for increasing initial spin rate. Table 2 shows the percent dissipation of kinetic energy for these six cases. An increase in R also increases the dissipation rate, because the fluid slug length is enlarged with constant β. As initial spin rate is increased, this simulation approaches correlation with Baines[8] for total time to stabilization. For the initial rate of 60 rad/min, a total projected stabilization time would be about 4.5 hr, as compared to 2.5 hr predicted by Baines.

Mean value of the nutation angle θ is illustrated qualitatively in Fig. 5. However, because of asymmetry of the body θ is an oscillatory quantity. After initial perturbation it will oscillate with increasing amplitude for some time, because the angular velocity vector is "precessing" from minor to major axis. This unstable oscillation will reach a peak and the envelope of oscillation will slowly start to converge to its final state. Figure 8 shows the general form of the θ envelope with destabilizing and stabilizing modes defined. This form, confirmed by the simulations, points out a problem of major concern. At the peak value of θ, as the destabilizing mode ends, it is possible that the mean value of θ may converge to π, rather than 0. Although this "ambiguity" did not occur for the model studied, it can be the result of other dissipation mechanisms which were not considered. This ambiguity was experienced by ATS-V and results in opposite spin and pointing in the retrofire direction. Resolution of this ambiguity problem must be obtained before practical application of AMAPS is possible.

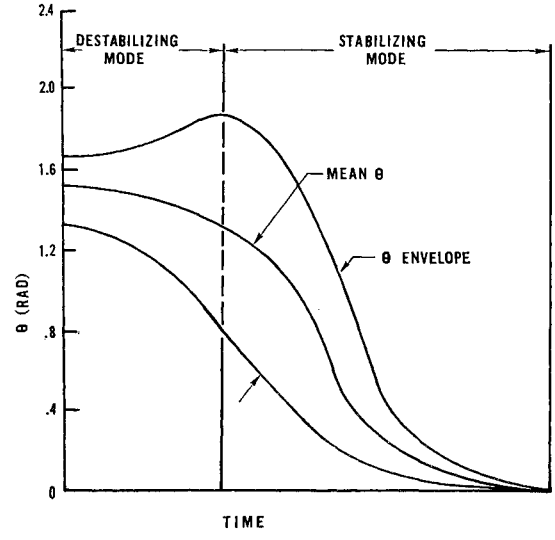

Fig. 8 Configuration for θ envelope of oscillation.

Conclusions

Although operational details have not been worked out, the AMAPS concept seems feasible and should result in significant reduction in deployment hardware and cost in many cases. Quantitative results are limited, but those obtained indicate axis transformation is easily accomplished before the first apogee. Furthermore, the discrete parameter model method seems to perform well for simple dissipation mechanisms.

References

[1] Likins, P. W. and Bouvier, H. K., "Attitude Control of Nonrigid Spacecraft," *Astronautics and Aeronautics*, Vol. 9, No. 5, May 1971, pp. 64–71.

[2] Bracewell, R. N. and Garriott, O. K., "Rotation of Artificial Earth Satellites," *Nature*, Vol. 182, No. 4638, Sept. 20, 1958, pp. 760–762.

[3] Fitzgibbon, D. P. and Smith, W. E., "Final Report on Study of Viscous Liquid Passive Wobble Dampers for Spinning Satellites," EM 11-14, June 1960, TRW Systems, Space Technology Lab., Redondo Beach, Calif.

[4] Kaplan, M. H. et al., "Dynamics and Control for Orbital Retrieval Operations Using the Space Shuttle," KSC-TR-1113, Vol. I, May 1971, NASA, pp. 175–201.

[5] Thomson, W. T. and Reiter, G. S., "Attitude Drift of Space Vehicles," *Journal of the Astronautical Sciences*, Vol. 7, No. 2, 1960, pp. 29–34.

[6] Meirovitch, L. and Nelson, H. D., "On the High-Spin Motion of a Satellite Containing Elastic Parts," *Journal of Spacecraft and Rockets*, Vol. 3, No. 11, Nov. 1966, pp. 1597–1602.

[7] Hazeltine, W. R., "Passive Damping of Wobbling Satellites: General Stability Theory and Example," *Journal of the Aerospace Sciences*, Vol. 29, No. 5, May 1962, pp. 543–549, 557.

[8] Baines, D. J., "A Satellite Rotational Kinetic Energy Dissipator," *Journal of Spacecraft and Rockets*, Vol. 6, No. 7, July 1965, pp. 850–853.

[9] Thomson, W. T., *Introduction to Space Dynamics*, Wiley, New York, 1961, pp. 111–113.

[10] Meirovitch, L., *Methods of Analytical Dynamics*, McGraw-Hill, New York, 1970, pp. 72–79.

JUNE 1972 J. SPACECRAFT VOL. 9, NO. 6

Pressurized Crack Behavior in Two-Dimensional Rocket Motor Geometries

E. C. FRANCIS*
United Technology Center, Sunnyvale, Calif.
AND
G. H. LINDSEY†
Naval Postgraduate School, Monterey, Calif.
AND
R. R. PARMERTER‡
University of Washington, Seattle, Wash.

A method is presented for evaluating two-dimensional crack behavior in rocket motor geometries for pressure loadings in which the pressure is applied directly to the crack surfaces. The experimental requirements associated with pressurizing the crack necessitated the application of pressure over the two-dimensional plane surface of the specimen. Analytical solutions are developed which include the side pressure and relate the stress intensity factors to the classical unpressurized situation. Stress intensity factors for the complex cracked rocket motor geometries were evaluated using finite element computer techniques based on strain energy methods. Comparison between analytical predictions using elastic fracture mechanics and experimental observations of a brittle epoxy was quite good for the three different geometries tested. The work has application in fracture analysis of solid propellant rocket grains and in pressure vessels containing partial-thickness cracks which emanate from the inside.

Nomenclature

A,B,C = star tip crack identification
a,b = internal, external grain radius
D = multiplicative factor
E = Young's modulus
G = general geometric function
h = outside case radius
K_I = stress intensity factor
p = pressure
r = radius
u = displacement
U = strain energy
γ = surface energy
Δ = increment
δ_{ij} = Kronecker delta
θ = angle
ν = Poisson's ratio
σ = stress

Subscripts and Superscripts

a,b,c,d,e,f = problem identification
i,j,k = tensor coordinates

Received June 16, 1971; revision received January 31, 1972. This work was supported by the Air Force Rocket Propulsion Laboratory, Edwards, Calif., under Contract F04611-69-C-0034. The authors wish to acknowledge the assistance of N. D. Walker Jr. in obtaining numerical solutions.

Index categories: Solid and Hybrid Rocket Engines; Computer Technology and Computer Simulation Techniques; Structural Static Analysis.

* Head, Propellant Properties Evaluation.
† Associate Professor of Aeronautics.
‡ Associate Professor of Aeronautics and Astronautics.